WORKING TITLE: UTILIZING INVARIANT MANIFOLDS OF CISLUNAR PERIODIC ORBITS FOR EFFICIENT DEEP SPACE TRANSFERS

by

Jonathan Richmond

A Thesis

Submitted to the Faculty of Purdue University

In Partial Fulfillment of the Requirements for the degree of

Master of Science in Aeronautics and Astronautics

School of Aeronautics and Astronautics

West Lafayette, Indiana

May 2024

THE PURDUE UNIVERSITY GRADUATE SCHOOL
STATEMENT OF COMMITTEE APPROVAL

Dr. Kathleen C. Howell, Chair

School of Aeronautics and Astronautics

Dr. Carolin Frueh

School of Aeronautics and Astronautics

Dr. Kenshiro Oguri

School of Aeronautics and Astronautics

Approved by:

Dr. Gregory A. Blaisdell

ADD DEDICATION

ACKNOWLEDGMENTS

ADD ACKNOWLEDGEMENTS

TABLE OF CONTENTS

LIST OF TABLES

LIST OF FIGURES

LIST OF SYMBOLS

Variables

a	Semimajor axis [km]
B	Barycenter
C	Jacobi constant
d_{SoI}	Sphere of influence gravitational ratio
E	Eccentric anomaly [rad (deg)]
$\mathcal{E}$	Specific mechanical energy [km^2/s^2]
e	Eccentricty
$\bar{\text{e}}$	Eccentricity vector in $\mathbb{R}^3$
$\bar{F}_g$	Gravitational force vector in $\mathbb{R}^3$ [kN]
G	Universal gravitational constant [kN*km^2/kg^2]
$\tilde{G}$	Normalized gravitational constant
g	Gravitational acceleration
$\bar{h}$	Specific angular momentum vector in $\mathbb{R}^3$ [km^2/s]
i	Inclination [rad (deg)]
L	Lagrange (equilibrium) point
l^*	Characteristic length [km]
M	Mean anomaly [rad (deg)]
m	Mass [kg]
m^* Characteristic mass [kg]	
n	Mean motion [rad/s (deg/s)]
$\tilde{n}$	Normalized mean motion
$\bar{n}$	Node vector in $\mathbb{R}^3$
P	Primary
$\mathbb{P}$	Period [s]
$\bar{Q}$	Inertial state vector in $\mathbb{R}^6$
$\bar{q}$	Rotating state vector in $\mathbb{R}^6$
$\bar{R}$	Inertial position vector in $\mathbb{R}^3$ [km]

r	Distance [kg]
$\bar{r}$	Position vector in $\mathbb{R}^3$ [km]
$\dot{\bar{r}}$	Velocity vector in $\mathbb{R}^3$ [km/s]
$\ddot{\bar{r}}$	Acceleration vector in $\mathbb{R}^3$ [km/s^2]
r_a	Radius of apoapsis [km]
r_p	Radius of periapsis [km]
s/c	Spacecraft
t	Time [s]
t^*	Characteristic time [s]
U	Pseudo-potential
v	Velocity [km/s]
v_r	Radial velocity [lm/s]
X	Position along the $\hat{X}$-axis in an inertial frame [km]
$\ddot{X}$	Acceleration along the $\hat{X}$-axis in an inertial frame [km/s^2]
x	Position along the $\hat{x}$-axis in a rotating frame
$\dot{x}$	Velocity along the $\hat{x}$-axis in a rotating frame
$\ddot{x}$	Acceleration along the $\hat{x}$-axis in a rotating frame
Y	Position along the $\hat{Y}$-axis in an inertial frame [km]
$\ddot{Y}$	Acceleration along the $\hat{Y}$-axis in an inertial frame [km/s^2]
y	Position along the $\hat{y}$-axis in a rotating frame
$\dot{y}$	Velocity along the $\hat{y}$-axis in a rotating frame
$\ddot{y}$	Acceleration along the $\hat{y}$-axis in a rotating frame
Z	Position along the $\hat{Z}$-axis in an inertial frame [km]
$\ddot{Z}$	Acceleration along the $\hat{Z}$-axis in an inertial frame [km/s^2]
z	Position along the $\hat{z}$-axis in a rotating frame
$\dot{z}$	Velocity along the $\hat{z}$-axis in a rotating frame
$\ddot{z}$	Acceleration along the $\hat{z}$-axis in a rotating frame
θ	True anomaly [rad (deg)]
μ	CR3BP mass ratio

μ_{2BP}	Two-body gravitational constant [kN*km^2/kg]
$\bar{P}$	Inertial position vector in $\mathbb{R}^3$
$\dot{\rho}$	Barycentric rotating velocity
$\bar{\rho}$	Barycentric rotating position vector in $\mathbb{R}^3$
$\dot{\bar{\rho}}$	Barycentric rotating velocity vector in $\mathbb{R}^3$
τ	Time
Ω	Right ascension of ascending node (RAAN) [rad (deg)]
ω	Argument of periapsis [rad (deg)]
$\bar{\omega}$	Angular velocity vector in $\mathbb{R}^3$
Coordinate Frames	
$\{\hat{X}, \hat{Y}, \hat{Z}\}$	Arbitrary inertial coordinate frame
$\{\hat{X}_{Ec}, \hat{Y}_{Ec}, \hat{Z}_{Ec}\}$	Ecliptic J2000 inertial coordinate frame
$\{\hat{x}, \hat{y}, \hat{z}\}$	Rotating coordinate frame

ABBREVIATIONS

2BP	2-Body Problem
BCR4BP	Bicircular Restricted 4-Body Problem
CR3BP	Circular Restricted 3-Body Problem
HFEM	High-fidelity ephemeris model
HR4BP	Hills Restricted 4-Body Problem
NAIF	Navigation and Ancillary Information Facility
QBCR4BP	Quasi-Bicircular Restricted 4-Body Problem
RAAN	Right ascension of ascending node
SoI	Sphere of influence

ABSTRACT

ADD ABSTRACT

1. INTRODUCTION

Experimenting with the available typographic conventions defined in the Purdue file: `pa-typographic-conventions.sty`: these include *Emph* *First* *Title* Keys `Literal` Menu Open menu > Preferences **`Shell.sh`**. Now let's try out a footnote[1], one of the fancy TODO notes , and more scary TODO , as well as a a todo error as well as a citation [1]. Note the TODO comments currently only show up in `quick` or `debug` modes (for now).

1.1 Subcaption / Cleveref Testing

Here is a very important and informative figure for Orion. You can see in Figure 1.1 that there is both Figure 1.1(a) and Figure 1.1(b)! There is also important information in Table 1.1. If you're confused, then Equation (1.1) should clarify things. Some other ways to put it: Equations (1.1) and (1.2) and Equations (1.1) to (1.3).

1.1.1 Important Math

$$\mathrm{e}^{\mathrm{i}\pi} + 1 = 0 \tag{1.1}$$

$$a^2 + b^2 = c^2 \tag{1.2}$$

$$\frac{df}{dt} = \lim_{h \to 0} \frac{f(t+h) - f(t)}{h} \tag{1.3}$$

1.1.2 Numbers/Units

Some of the number formats available: -10^{10}. 2×4. 10 to 11. 12.3°.

Experimenting with the siunits package: $8\ \mathrm{kg\,m\,s^{-2}}$. 9N. $2.3 \times 10^{27}\,\mathrm{kg}$. $1.345\,\frac{\mathrm{C}}{\mathrm{mol}}$.

[1]↑I'm a footnote!

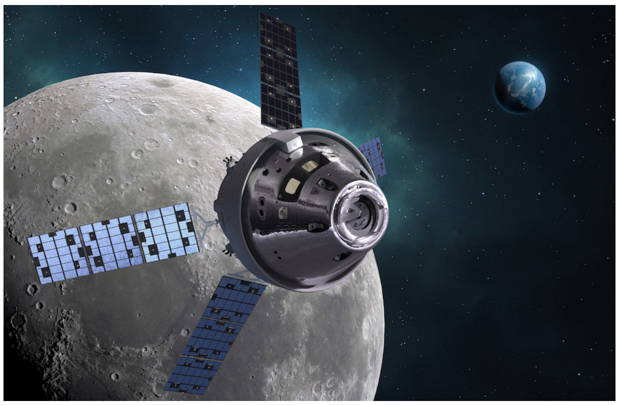

(a) Orion 1

(b) Orion 2

Figure 1.1. Two images of Orion: (a) and (b).

Table 1.1. Sample Table

Sample	Table
x	2

A subsubsection

A subsubsection for testing out the table of contents

A paragraph

What happens for a paragraph in the table of contents?

1.1.3 Custom variables

Variables can be defined as functions in t0-template › te4-custom-variables.tex

The rotating x axis is clearly the best of all axes. But even better is the $\boldsymbol{x}$ vector and the $\hat{x}$ direction! See the appenix in Debug mode for details

1.1.4 Custom colors

There are a variety of available colors from Purdue's branding[2] like: Boilermaker Gold, Rush. This example document also include the Tableau colors[3]. For example, tab-blue and tab-red.

1.1.5 Acronyms

Acronyms handled through `glossaries`, and defined in t0-template › te6-acronyms.tex. For example, the first time we will refer to the Circular Restricted Three Body Problem (CR3BP), and in the future only say CR3BP.

[2]↑see https://marcom.purdue.edu/our-brand/visual-identity/
[3]↑used in matplotlib - https://matplotlib.org/3.4.1/gallery/color/named_colors.html

2. DYNAMICAL MODELS

This analysis relies on the utilization of two primary dynamical models: The Two-Body Problem (2BP) and the Circular Restricted Three-Body Problem (CR3BP). The 2BP serves as a model for spacecraft dynamics when their motion is solely governed by the gravitational influence of a single body, primarily applied to the study of heliocentric arcs within this investigation. In cases where the dynamics are significantly influenced by the gravitational forces of two bodies, as exemplified in Sun-planet or the Earth-Moon systems, the CR3BP offers a more accurate description of the spacecraft's motion.

2.1 Coordinate Frames

In this investigation, Cartesian coordinate frames are employed to represent three-dimensional vector quantities. These frames may either remain fixed in space (inertial) or rotate about the origin at a constant angular rate (rotating). The choice of coordinate frame depends on the specific application as it can be advantageous to position the origin at the center of mass of the system (barycenter) or align it with a primary body of interest.

2.1.1 Barycentric Rotating and Inertial Frames

In a CR3BP system, the motion of a spacecraft is best depicted within a rotating frame with its origin at the system barycenter. The $\hat{x}$-axis is defined to extend from the barycenter toward the smaller primary body, while the $\hat{z}$-axis aligns with the sytem's angular momentum vector. Completing the triad, the $\hat{y}$-axis is established as $\hat{y} = \hat{z} \times \hat{x}$. This frame rotates about the barycenter at a constant angular rate identical to that of the primary bodies.

Additionally, an arbitrary barycentric inertial frame can be similarly defined using the rotating axes at a specific instance in time, denoted as $\hat{X}$, $\hat{Y}$, and $\hat{Z}$. As time progresses, the inertial frame remains fixed in space, whereas the rotating frame revolves around the shared origin with the primaries. In Figure 2.1, the barycentric $\{\hat{x}, \hat{y}, \hat{z}\}$ rotating frame and $\{\hat{X}, \hat{Y}, \hat{Z}\}$ inertial frames for an example CR3BP system are illustrated, with their common origin centered at the barycenter of the primaries, P_1 and P_2. The angle between the two frames is denoted here by θ and it increases at a constant rate of n. It is important to note that both the $\hat{Z}$- and $\hat{z}$-axes adhere to the right-hand frame convention, pointing out of the page.

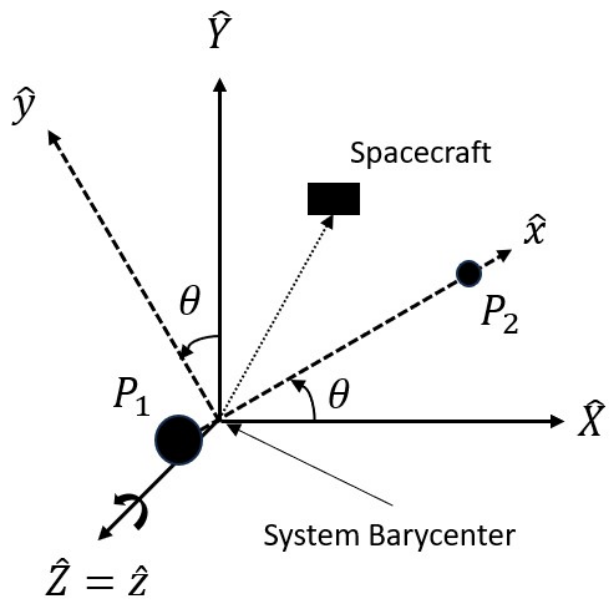

Figure 2.1. Barycentric rotating and inertial frames in a CR3BP system.

2.1.2 The Ecliptic J2000 Primary-Centered Inertial Frame

A commonly used primary-centered inertial frame is the Ecliptic J2000. As the name implies, this frame is established with its origin at the center of a primary body, and the Sun-Earth orbital plane on January 1, 2000 as the $\hat{X}_{Ec}\hat{Y}_{Ec}$-plane. The $\hat{X}_{Ec}$-axis is directed towards the vernal equinox, which is the line of intersection between the Earth's equatorial and ecliptic planes on January 1, 2000. The $\hat{Z}_{Ec}$-axis is orthogonal to the ecliptic plane, and the $\hat{Y}_{Ec}$-axis completes the triad, defined as $\hat{Y}_{Ec} = \hat{Z}_{Ec} \times \hat{X}_{Ec}$.

Since the frame is centered on a primary, it is applicable to both the 2BP and CR3BP, making it also valuable for patched dynamical models. The construction of this coordinate frame, as depicted in Figure 2.2, is computed using the Navigation and Ancillary Information Facility's (NAIF) SPICE ephemeris toolkit[2].

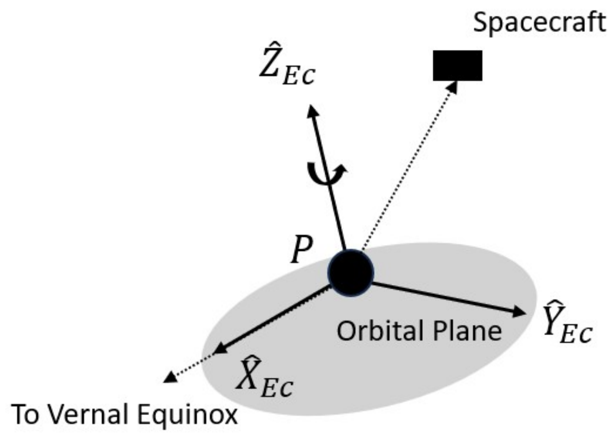

Figure 2.2. Earth-centered Ecliptic J2000 inertial frame.

2.2 The Two-Body Problem

This investigation treats the motion of spacecraft in heliocentric space, specifically when they are far from planets and moons, as a Two-Body Problem, governed by a single gravitational force. This section provides a brief overview of key aspects of 2BP dynamics, Keplerian orbital elements, and Kepler's Equation. For a more comprehensive derivation of the 2BP, refer to Chapters 1 and 2 of Vallado's *Fundamentals of Astrodynamics and Applications*[3]. Additionally, Canales highlights the background information relevant for understanding the transfer methodologies presented in this analysis[4].

2.2.1 Equations of Motion

The 2BP involves two point masses—a primary body and a spacecraft—that exert gravitational forces on each other. Since no external forces act on this system, the center of mass of the bodies moves at a constant velocity and serves as the origin for an inertial coordinate frame. In this inertial frame, the gravitational force that the primary body exerts on the spacecraft, denoted as $\bar{F}_{g_{P\to s/c}}$, is expressed as:

$$\bar{F}_{g_{P\to s/c}} = -\frac{Gm_P m_{s/c}}{r^3_{P\to s/c}}\bar{r}_{P\to s/c}, \tag{2.1}$$

where G is the universal gravitational constant (6.67384x10^{-20} kN*km^2/kg^2), m_P and m_S are the masses of the primary body and spacecraft, respectively, $r_{P\rightarrow s/c}$ is the distance from the primary body to the spacecraft, and $\bar{r}_{P\rightarrow s/c} = \bar{r}_{s/c} - \bar{r}_P$ is the position vector from the primary body to the spacecraft in the inertial frame, as illustrated in Figure 2.3.

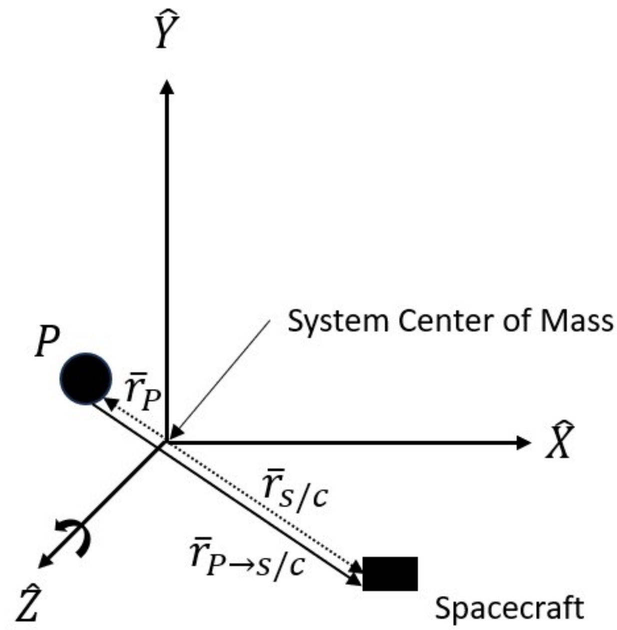

Figure 2.3. Two-body problem in a barycentric inertial frame.

Assuming that the mass of the spacecraft is negligible compared to the mass of the primary body, the nonlinear relative equation of motion for the 2BP is derived[3], [4]:

$$\ddot{\bar{r}}_{P\rightarrow s/c} = -\frac{\mu_{2BP}}{r^3_{P\rightarrow s/c}}\bar{r}_{P\rightarrow s/c}, \tag{2.2}$$

where $\ddot{\bar{r}}_{P\rightarrow s/c}$ is the inertial acceleration of the spacecraft relative to the primary body and $\mu_{2BP} = Gm_P$. This vector equation can also be expressed as $\hat{X}$, $\hat{Y}$, and $\hat{Z}$ scalar equations in the inertial frame:

$$\ddot{X} = -\frac{\mu_{2BP}}{r^3_{P\rightarrow s/c}}(X_{s/c} - X_P), \tag{2.3}$$

$$\ddot{Y} = -\frac{\mu_{2BP}}{r^3_{P\rightarrow s/c}}(Y_{s/c} - Y_P), \tag{2.4}$$

$$\ddot{Z} = -\frac{\mu_{2BP}}{r^3_{P\rightarrow s/c}}(Z_{s/c} - Z_P). \tag{2.5}$$

2.2.2 Conic Sections

Instead of relying on numerical propagation of the nonlinear equations of motion, spacecraft motion in the 2BP can be effectively represented analytically using conic sections. This section provides a concise overview of conic motion in the 2BP.

Two essential constants characterize conic orbits: specific angular momentum $\bar{h}$ and specific mechanical energy $\mathcal{E}$:

$$\bar{h} = \bar{r}_{P\to s/c} \times \dot{\bar{r}}_{P\to s/c}, \tag{2.6}$$

$$\mathcal{E} = \frac{v^2_{P\to s/c}}{2} - \frac{\mu_{2BP}}{r_{P\to s/c}}, \tag{2.7}$$

where $v_{P\to s/c} = ||\dot{\bar{r}}_{P\to s/c}||_2$ is the spacecraft velocity in the inertial frame relative to the primary body.

Kepler's first law, asserting that orbital motion is conic, provides the trajectory equation for the 2BP:

$$r_{P\to s/c} = \frac{a(1-\mathrm{e}^2)}{1+\mathrm{e}\cos(\theta)}, \tag{2.8}$$

where a represents the orbit semimajor axis, e is the orbit eccentricity, and θ denotes the orbit true anomaly. These three elements will be elaborated upon in a later subsection. Equation (2.8) can also be employed to compute the periapsis and apoapsis distances, r_p and r_a respectively:

$$r_p = a(1-\mathrm{e}), \tag{2.9}$$

$$r_a = a(1+\mathrm{e}). \tag{2.10}$$

The eccentricity can also be used to determine the type of conic section:

- $\mathrm{e} = 0$: Circular orbit (a special case of an ellipse).
- $0 < \mathrm{e} < 1$: Elliptical orbit.
- $\mathrm{e} = 1$: Parabola.
- $\mathrm{e} > 1$: Hyperbola.

This investigation focuses on circles and ellipses with $0 \leq \mathrm{e} < 1$.

In similar fashion, Kepler's third law provides the orbit period $\mathbb{P}$ and, consequently, the mean motion n:

$$\mathbb{P} = 2\pi\sqrt{\frac{a^3}{\mu_{2BP}}}, \tag{2.11}$$

$$n = \frac{2\pi}{\mathbb{P}} = \sqrt{\frac{\mu_{2BP}}{a^3}}. \tag{2.12}$$

2.2.3 Keplerian Orbital Elements

Instead of specifying the six-dimensional state of a spacecraft in a 2BP elliptical orbit using Cartesian coordinates, six orbital elements can be employed to articulate the size, shape, orientation, and current location along the orbit. In addition to the semimajor axis a and eccentricity e, which were introduced earlier and describe the size and shape of the ellipse, three angles characterize the orientation of the orbit with respect to an inertial frame, as depicted in Figure 2.4:

- Inclination i signifies the tilt of the orbital plane relative to the inertial $\hat{X}_{Ec}\hat{Y}_{Ec}$-plane.
- Right ascension of the ascending node (RAAN) Ω denotes the angle between the $\hat{X}_{Ec}$-axis and the ascending node, where the orbit crosses the $\hat{X}_{Ec}\hat{Y}_{Ec}$-plane in the positive $\hat{Z}_{Ec}$ direction.
- Argument of periapsis ω is the angle between the ascending node and the periapsis.

Finally, the true anomaly θ defines the spacecraft's position relative to the orbit's periapsis.

Cartesian state to Keplerian orbital elements

To convert from a Cartesian state vector to Keplerian orbital elements, start by calculating the inclination from angular momentum:

$$\mathrm{i} = \arccos\left(\frac{h_Z}{||\bar{h}||}\right) \tag{2.13}$$

Using the node vector $\bar{n}$:

$$\bar{n} = \hat{Z}_{Ec} \times \bar{h}, \tag{2.14}$$

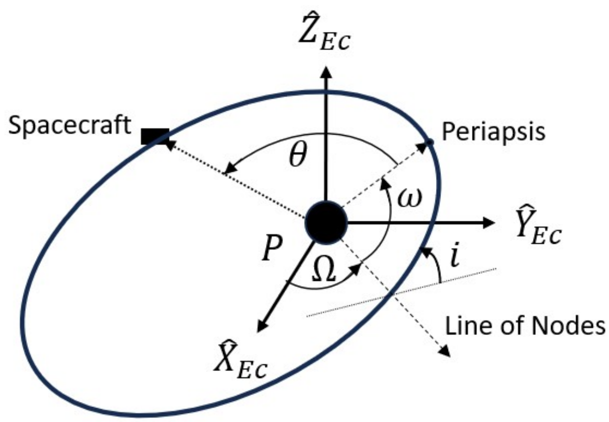

Figure 2.4. Orientation and location along an orbit in an inertial frame using Keplerian orbital elements.

the RAAN becomes:

$$\Omega = \begin{cases} \arccos(\frac{n_X}{||\bar{n}||}) & n_Y \geq 0 \\ 2\pi - \arccos(\frac{n_X}{||\bar{n}||}) & n_Y < 0 \end{cases}. \tag{2.15}$$

The eccentricity vector $\bar{\mathrm{e}}$ is also calculated from the angular momentum:

$$\bar{\mathrm{e}} = \frac{\dot{\bar{r}}_{P\to s/c} \times \bar{h}}{\mu_{2BP}} - \frac{\bar{r}_{P\to s/c}}{r_{P\to s/c}}, \tag{2.16}$$

and

$$\mathrm{e} = ||\bar{\mathrm{e}}||. \tag{2.17}$$

The remaining three orbital elements are calculated as follows:

$$a = \frac{||\bar{h}||}{\mu_{2BP}(1 - \mathrm{e}^2)}, \tag{2.18}$$

$$\omega = \begin{cases} \arccos(\frac{\bar{n}\cdot\bar{\mathrm{e}}}{||\bar{n}||\mathrm{e}}) & \mathrm{e}_Z \geq 0 \\ 2\pi - \arccos(\frac{\bar{n}\cdot\bar{\mathrm{e}}}{||\bar{n}||\mathrm{e}}) & \mathrm{e}_Z < 0 \end{cases}, \tag{2.19}$$

$$\theta = \begin{cases} \arccos(\frac{\bar{\mathrm{e}}\cdot\bar{r}_{P\to s/c}}{\mathrm{e}r_{P\to s/c}}) & v_r \geq 0 \\ 2\pi - \arccos(\frac{\bar{\mathrm{e}}\cdot\bar{r}_{P\to s/c}}{\mathrm{e}r_{P\to s/c}}) & v_r < 0 \end{cases}, \tag{2.20}$$

where

$$v_r = \frac{\dot{\bar{r}}_{P\rightarrow s/c} \cdot \bar{r}_{P\rightarrow s/c}}{r_{P\rightarrow s/c}}. \tag{2.21}$$

Keplerian orbital elements to Cartesian state

Similarly, the Cartesian state vector can be obtained from the Keplerian orbital elements. First, the eccentric anomaly E is needed, which is the angle made by the eccentricity vector pointing to perapsis and the vector from the center of the ellipse to the point directly above the spcacecraft location (perpendicular to the eccentricity vector) on an auxiliary circle drawn tangent to the ellipse. The eccentric anomaly and the auxiliary circle are illustrated in Figure 2.5, along with the eccentricity vector and semimajor axis.

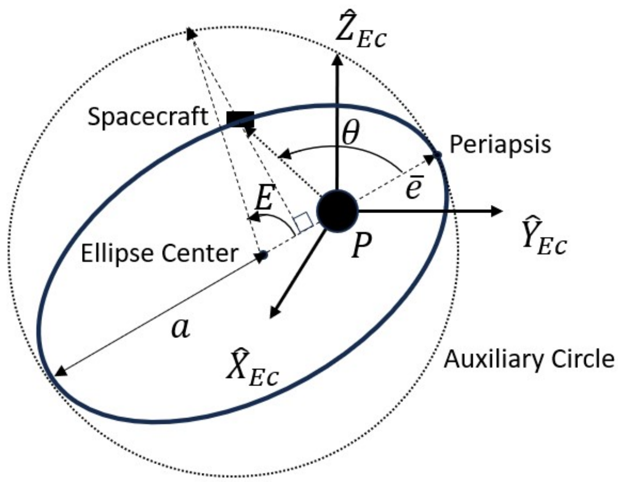

Figure 2.5. Definition of eccentric anomaly and the auxiliary circle.

The eccentric anomaly can be related to the true anomaly,

$$E = \arctan(\frac{\sqrt{1-\mathrm{e}^2}\sin(\theta)}{\mathrm{e}+\cos(\theta)}), \tag{2.22}$$

which can then be used to calculate the distance from the primary:

$$r_{P\rightarrow s/c} = a(1 - \mathrm{e}\cos(E)). \tag{2.23}$$

This can be used to generate position and velocity magnitude vectors:

$$\bar{r}_0 = \begin{bmatrix} r_{P\to s/c}\cos(\theta) \\ r_{P\to s/c}\sin(\theta) \\ 0 \end{bmatrix}, \tag{2.24}$$

$$\dot{\bar{r}}_0 = \sqrt{\frac{\mu_{2BP}a}{r_{P\to s/c}}}\begin{bmatrix} -\sin(E) \\ \sqrt{1-\mathrm{e}^2}\cos(E) \\ 0 \end{bmatrix}. \tag{2.25}$$

These vectors will need to be rotated relative to the inertial frame axes according to the inclination, RAAN, and argument of periapsis:

$$C = \begin{bmatrix} \cos(\Omega)\cos(\omega) - \cos(\mathrm{i})\sin(\Omega)\sin(\omega) & -\cos(\Omega)\sin(\omega) - \cos(\mathrm{i})\sin(\Omega)\cos(\omega) & 0 \\ \sin(\Omega)\cos(\omega) + \cos(\mathrm{i})\cos(\Omega)\sin(\omega) & -\sin(\Omega)\sin(omega) + \cos(\mathrm{i})\cos(\Omega)\cos(\omega) & 0 \\ \sin(\mathrm{i})\sin(\omega) & \sin(\mathrm{i})\cos(\omega) & 0 \end{bmatrix}, \tag{2.26}$$

$$\bar{r}_{P\to s/c} = C\bar{r}_0, \tag{2.27}$$

$$\dot{\bar{r}}_{P\to s/c} = C\dot{\bar{r}}_0. \tag{2.28}$$

2.2.4 Kepler's Equation

If the difference in true anomaly between two points on an orbit is known, Kepler's equation becomes a valuable tool for calculating the time-of-flight between these points. The mean anomaly M serves as a measure of how much of the orbit has been traversed past periapsis with respect to time:

$$M = \frac{2\pi(t - t_p)}{\mathbb{P}}, \tag{2.29}$$

where $(t - t_p)$ represents the time since periapsis.

Kepler's equation estabishes a connection between the mean and eccentric anomalies, thereby linking the eccentric anomaly to time:

$$M = E - \mathrm{e}\sin(E). \tag{2.30}$$

To determine eccentric anomalies given corresponding true anomalies, employ Equation (2.22), and subsequently, using Kepler's equation (Equation (2.30)), convert them to mean anomalies. The difference in mean anomalies with Equation (2.29) provides the time-of-flight between the two points along the orbit.

2.3 The Circular Restricted Three-Body Problem

When a spacecraft is significantly impacted by the gravitational force of two celestial bodies the Circular Restricted 3-Body Problem better approximates the spacecraft's motion compared to two-body problems. Therefore, this investigation uses the CR3BP to model the Earth-Moon and Sun-planet systems when appropriate. The CR3BP is an autonomous model (its dynamics are time-invariant) that provides insight into the dynamical structures present in the system without some of the complexities of a higher-fidelity ephemeris model.

2.3.1 Equations of Motion

The CR3BP consisits of three primary bodies, two celestial bodies and a masless spacecraft. The two celestial bodies exert gravitational forces on each other and the satellite; however, the satellite does not affect the other two bodies.

The two celestial bodies are treated as point masses and assumed to move in circular orbits, with a constant angular velocity, around their barycenter B. Assuming that no other forces are acting on the system, B can be considered an inertial point and similar to the 2BP, Newton's Laws can be expressed relative to that point. Unlike the 2BP, there is currently no analytical solution to represent the dynamics of the CR3BP. Consequently, all trajectories in this model must be numerically propagated in time using nonlinear, coupled equations of motion.

It is also useful and common practice to represent these equations and visualize them in a barycentric rotating coordinate frame, $\{\hat{x}, \hat{y}, \hat{z}\}$, as shown by the dashed lines in Figure 2.1 and described in Section 2.1. In this frame, the two celestial primaries remain fixed, while the spacecraft moves relative to them in three-dimensional configuration space.

A single mass ratio μ characterizes a CR3BP system:

$$\mu = \frac{m_2}{m_1 + m_2}, \tag{2.31}$$

where m_1 and m_2 are the masses of the larger and smaller celestial primaries, respectively. In the barycentric rotating frame, P_1 is located at $x = -\mu$ and P_2 is located at $x = 1 - \mu$. Using this parameter, a pseudo-potential function U describes the gravitational forces on the system expressed in the barycentric rotating frame:

$$U = \frac{1}{2}(x^2 + y^2) + \frac{1-\mu}{d} + \frac{\mu}{r}, \tag{2.32}$$

$$d = \sqrt{(x+\mu)^2 + y^2 + z^2}, \tag{2.33}$$

$$r = \sqrt{(x-1+\mu)^2 + y^2 + z^2}, \tag{2.34}$$

where here, d and r are the distances from P_1 and P_2, respectively. From the pseudo-potential, the scalar nonlinear equations of motion are expressed in the barycentric rotating frame:

$$\ddot{x} = 2\dot{y} + \frac{\partial U}{\partial x} = 2\dot{y} + x - \frac{(1-\mu)(x+\mu)}{d^3} - \frac{\mu(x-1+\mu)}{r^3}, \tag{2.35}$$

$$\ddot{y} = -2\dot{x} + \frac{\partial U}{\partial y} = -2\dot{x} + y - \frac{(1-\mu)y}{d^3} - \frac{\mu y}{r^3}, \tag{2.36}$$

$$\ddot{z} = \frac{\partial U}{\partial z} = -\frac{(1-\mu)z}{d^3} - \frac{\mu z}{r^3}. \tag{2.37}$$

Many authors provide detailed derivations for these equations of motion; one useful reference is Zimovan's Ph.D. dissertation[5].

2.3.2 Nondimensionalized Values

Since planetary systems deal with massive distance and velocity scales, it is often helpful in computations to use normalized length, time, and mass values with nondimensional units. Each CR3BP system has characteristic values that are used in this normalization process:

- Characteristic length l^* is the distance between the celestial primaries.

- Characteristic time t^* is selected so that the mean motion of these primaries is unity ($\tilde{n} = 1$). This results in the primaries having circular orbital periods of 2π nondimensional units.

- Characteristic mass m^* is the sum of the masses of these two bodies.

These definitions result in the following equations:

$$l^* = r_{12}, \tag{2.38}$$

$$m^* = m_1 + m_2, \tag{2.39}$$

$$t^* = \sqrt{\frac{l^{*3}}{Gm^*}}, \tag{2.40}$$

$$\tilde{G} = G\frac{l^{*3}}{m^* t^{*2}} = 1, \tag{2.41}$$

which are used to normalize all dimensional values in the problem.

2.3.3 Equilibrium Points

In the barycentric rotating frame, there are five equilibrium points (also called libration or Lagrange points) where there is no net acceleration (i.e., the pseudo-potential acceleration is balanced by the centrifugal acceleration). Thus, a spacecraft at these positions with no initial velocity would remain stationary in this model. All five Lagrange points lie in the xy-plane. Three Lagrange points lie along the axis of the two celestial primaries and are called the collinear equilibrium points: L_1 is between the two bodies, L_2 is past the smaller body, and L_3 is past the larger body. A Newton-Raphson algorithm can be used to find the location of these points for a given mass ratio. L_4 and L_5 are equilateral equilibrium points because they form equilateral triangles with the primary bodies. Their locations can be determined through geometric relationships. The energy level (or corresponding Jacobi constant, introduced in the next section) increases through points 1-4 (L_4 and L_5 are at the same energy level). Figure 2.6 shows the layout of the Lagrange points in a generic CR3BP barycentric rotating frame.

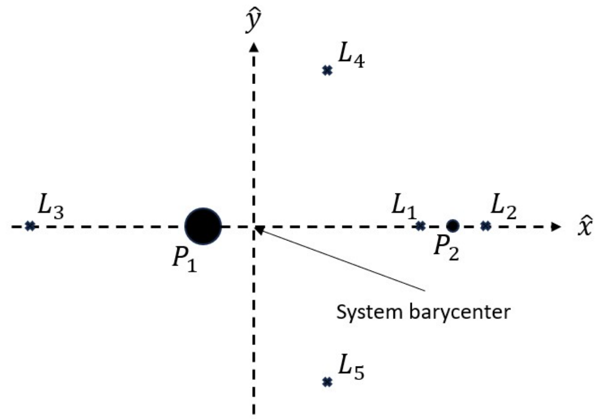

Figure 2.6. CR3BP barycentric rotating frame with Lagrange points.

2.3.4 Jacobi Constant

One reason that the CR3BP does not have a closed-form analytical solution like the 2BP is there are not enough integrals of the motion, at least that have been discovered to date. However, there is one such constant of the motion in the rotating frame, denoted as the Jacobi constant, and it proves useful as an analogy to energy. The derivation is as follows[5]:

$$\nabla U \cdot \dot{\bar{\rho}} = \frac{\partial U}{\partial x}\dot{x} + \frac{\partial U}{\partial y}\dot{y} + \frac{\partial U}{\partial z}\dot{z} = (\ddot{x} - 2\dot{y})\dot{x} + (\ddot{y} + 2\dot{x})\dot{y} + \ddot{z}\dot{z}, \tag{2.42}$$

where $\dot{\bar{\rho}}$ is the rotating velocity vector. The middle of Equation (2.42) is equivalent to the total nondimensional time derivative of the pseudo-potential:

$$\frac{dU}{d\tau} = \ddot{x}\dot{x} + \ddot{y}\dot{y} + \ddot{z}\dot{z}, \tag{2.43}$$

where τ is nondimensional time. Integrating and rearranging this equation provides the Jacobi constant as a function of rotating position and velocity:

$$C = 2U - \dot{\rho}^2, \tag{2.44}$$

where C is the Jacobi constant.

This definition of the Jacobi constant is consistent with the Hamiltonian of the system, which is time-invariant in the CR3BP[6]. Note also that as the Jacobi constant increases, the energy of the trajectory decreases.

2.4 Patched Dynamical Models

A variety of methods exist to model the gravitational forces of three (or more) celestial bodies in dynamical systems. While a high-fidelity ephemeris model (HFEM) provides the best accuracy, there are models that utilize simplifying assumptions to reduce computations and gain more insight into the dynamics of the system while maintaining adequate fidelity. For including all of the bodies in one model, there exist several 4-body problems that differ in layout, coherency, and fidelity. Some of the more prominent options are the Bicircular Restricted 4-Body Problem (BCR4BP)[7], Hills Restricted 4-Body Problem (HR4BP)[8], and Quasi-Bicircular Restricted 4-Body Problem (QBCR4BP)[9]. A different approach, and the one used in this investigation, is to patch together 2BP and CR3BP models to build a larger model to represent the dynamics. Two such patched models are outlined here.

2.4.1 The Patched 2BP-CR3BP Model

A patched 2BP-CR3BP model is used to describe trajectories as they move between CR3BP systems via a 2BP system. An example from this investigation is leaving the Sun-Earth CR3BP into heliocentric space (modeled as a 2BP) before entering the Sun-Mars CR3BP. While the spacecraft is near a planet, it is modeled in the Sun-planet CR3BP. But once it reaches a specified distance from that planet, it is modeled instead using Keplearian 2BP motion around the Sun[4]. The interface location between the two models is called the sphere of influence (SoI) since it represents where the gravitational influence of the planet becomes negligible compared to that of the Sun.

Trajectories computed in this model are best represented by using an inertial coordinate frame, centered on the focus of the 2BP, the Sun in this example. In this investigation, trajectories in the 2BP-CR3BP patched model are shown in the Sun-centered Ecliptic J2000 Inertial Frame, as described in Section 2.1.2. Although the Sun-Earth CR3BP is coplanar with this inertial frame, the Sun-Mars CR3BP system is not and Mars is considered to ve located at its respective orbital inclination. The XY-projection of an example 2BP-CR3BP patched model system is shown in Figure 2.7.

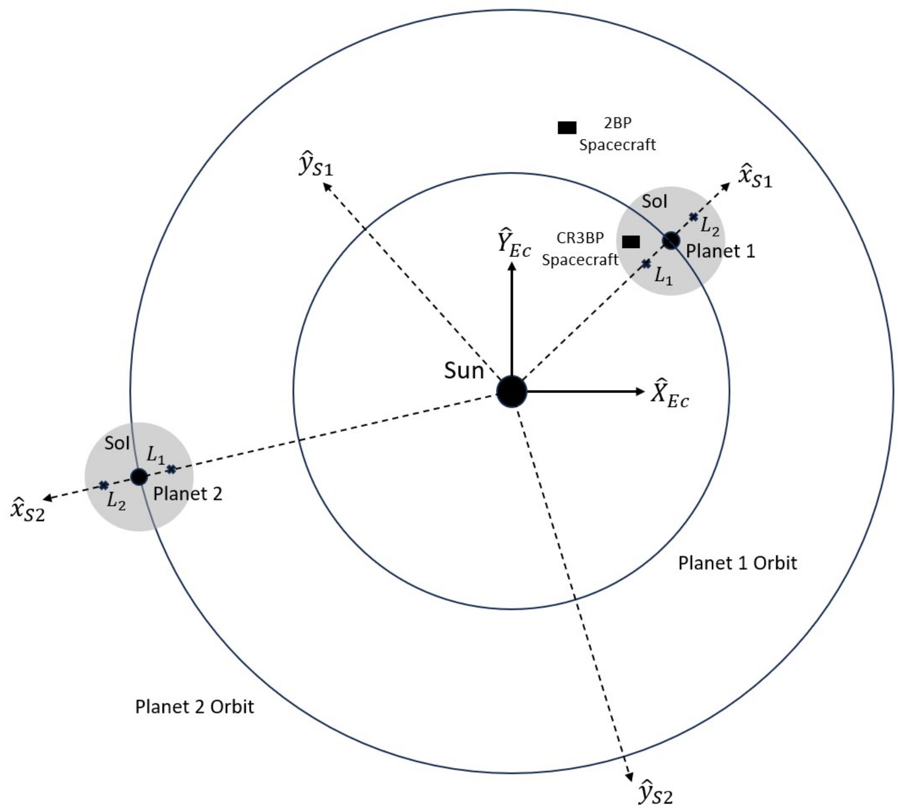

Figure 2.7. XY-Projection of the Patched 2BP-CR3BP Model

The radius of the SoI is a design parameter dependent on the application. For this patched model, an SoI is desired such that CR3BP periodic orbits around the Lagrange points are included. By defining a gravitational ratio:

$$d_{SoI} = \frac{g_2}{g_1}, \tag{2.45}$$

where g_{i} is the gravitational acceleration of the respective primary body at a specified location, an SoI radius from the planet can be chosen so that $d_S oI$ is sufficiently small, i.e., the osculating (instantaneous) orbital elements remain near constant in the CR3BP[4].

2.4.2 The Blended CR3BP Model

Two CR3BP models can be blended together to form a 4-body model if one of the primary bodies is present in both models. For example, a Sun-Earth CR3BP can be blended with an Earth-Moon CR3BP to form a Sun-Earth-Moon 4-body problem (here, the Earth is the common primary). This method incorporates the difference in inclinations between the two CR3BP models, but is now a time-dependent model[10]. Similar to the patched 2BP-CR3BP model, the boundary between the two models is at an SoI, now around the smaller primary of the smaller CR3BP model (the Moon in this example).

Unlike the patched model above, this model is best represented in the barycentric rotating frame of the larger CR3BP model (the Sun-Earth rotating frame in this example). Since the blended model is time-dependent, the portion of the trajectory computed in the smaller CR3BP will be shifted when represented in the larger model depending on the epoch. The xy-projection of an example blended system is shown in Figure 2.8.

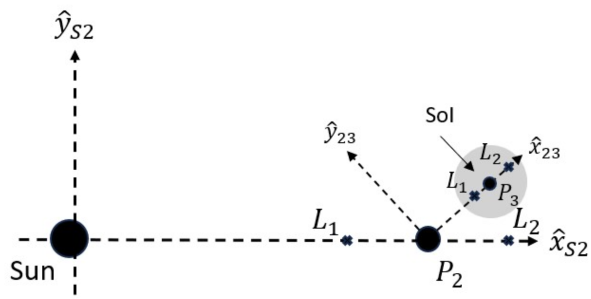

Figure 2.8. xy-Projection of the Blended CR3BP Model

The SoI radius used for the blended model is different from that used for the patched model. As mentioned before, this SoI is centered around the second primary of the smaller system and the gravitational accelerations being compared are the first primary of the larger system and the smaller primary of the second system (e.g., the Sun and the Moon). A blended CR3BP SoI radius is defined as:

$$r_{SoI} = l_{12}^{*}(\frac{m_3}{m_1})^{2/5}, \tag{2.46}$$

where the primaries are numbered in order of decreasing mass[11].

2.5 Coordinate Frame Transformations

Since the patched and blended models used in this investigation use a variety of models centered around different bodies, it is helpful to be able to view any trajectories in multiple reference frames. As mentioned previously, reference frames can be inertial or rotating, and an important component of interplanetary trajectory design is the ability to transform states and trajectories between these two types of frames. A few representative example coordinate frame transformations follow.

2.5.1 Barycentric Rotating Frame - Primary-Centric Arbitrary Inertial Frame

Most trajectories in a CR3BP are constructed in the barycentric rotating frame where Equation (2.35)-Equation (2.37) are defined (see Figure 2.1). However, it can also be beneficial to view these in an inertial frame centered on one of the primary gravitational bodies. An arbitrary inertial frame can be defined where the inertial unit vectors $\{\hat{X}, \hat{Y}, \hat{Z}\}$ are equivalent to the rotating unit vectors $\{\hat{x}, \hat{y}, \hat{z}\}$ at time t_0 (although the frame centers may be in different locations).

The following steps will transform (nondimensionalized) states from the barycentric rotating frame to a primary-centric arbitrary inertial frame:

1. Translate the position states from barycentric to primary-centric:

$$\bar{\rho}_{P\to s/c} = \bar{\rho}_{s/c} - \bar{\rho}_P. \tag{2.47}$$

2. Rotate the states depending on time since t_0

   Recall that the mean motion n of the rotating frame is constant. When nondimensionalized in the CR3BP, $\tilde{n} = 1$ and therefore the rtoation angle is just $\tau - \tau_0$. Since the

$\hat{z}$- and $\hat{Z}$-axes coincide for an arbitrary inertial frame, a simple rotation matrix can be used to rotate the position states:

$$\bar{P} = \begin{bmatrix} \cos(\tau - \tau_0) & -\sin(\tau - \tau_0) & 0 \\ \sin(\tau - \tau_0) & \cos(\tau - \tau_0) & 0 \\ 0 & 0 & 1 \end{bmatrix} \bar{\rho} = {}^{I}C^{R}\bar{\rho}, \tag{2.48}$$

where $\bar{\rho}$ is the rotating position and $\bar{P}$ is the inertial position.

Basic kinematics can be used to compute the velocity in the rotating frame relative to an inertial observer:

$$\frac{{}^{I}d\bar{\rho}}{d\tau} = \frac{{}^{R}d\bar{\rho}}{d\tau} + {}^{I}\bar{\omega}^{R} \times \bar{\rho} = \dot{\bar{\rho}} + \hat{z} \times \bar{\rho}, \tag{2.49}$$

where ${}^{I}\bar{\omega}^{R} = \tilde{n}\hat{z}$ is the angular velocity relating the two frames. Therefore:

$$\frac{{}^{I}d\bar{\rho}}{d\tau} = (\dot{x} - y)\hat{x} + (\dot{y} + x)\hat{y} + \dot{z}\hat{z}. \tag{2.50}$$

Using the rotation matrix ${}^{I}C^{R}$ from Equation (2.48), Equation (2.50) can be written in matrix from and combined with the position rotation to achieve full state rotation:

$$\bar{Q} = \begin{bmatrix} {}^{I}C^{R} & \bar{0} \\ {}^{I}\dot{C}^{R} & {}^{I}C^{R} \end{bmatrix} \bar{q}, \tag{2.51}$$

where $\bar{q}$ is the rotating state and $\bar{Q}$ is the inertial state.

3. Dimensionalize the states if desired (see Section 2.3.2).

To transform a primary-centric arbitrary inertial state to a barycentric rotating state, just reverse the above states (nondimensionalizing if necessary) and invert the state rotation matrix.

2.5.2 Barycentric Rotating Frame - Ecliptic J2000 Inertial Frame

When desigining a trajectory across multiple systems, it is often useful to view each part of the trajectory in a common inertial reference frame. In this investigation, the Earth

Ecliptic J2000 inertial frame, introduced in Section 2.1.2 (Figure 2.2), is used as the common frame for interplanetary trajectories.

The transformation between barycentric rotating frame states and a primary-centric Ecliptic J2000 inertial frame states follows a similar process to the arbitrary inertial frame. However, since this frame is defined by a particular epoch (January 1, 2000), the frame rotation is epoch-dependent:

1. To properly compare the rotating frame to the Ecliptic J2000 inertial frame, the location of the second primary in its orbit at each epoch of the trajectory is needed. This is obtained by retrieving the orbital elements of the second primary at a selected initial epoch from SPICE[2]. These orbital elements are then modified to match the CR3BP orbit assumptions ($a = l^*$ and e $= 0$). Since the mean motion/angular velocity in the CR3Bp is constant at $\tilde{n} = 1$:
$$\theta = \tau - \tau_0 + \theta_0, \tag{2.52}$$
where θ_0 is the true anomaly at the initial epoch $t - 0$ obtained from SPICE. These updated orbital elements are then used to calculate the full state vector (in dimensional units) of the second primary relative to the first using Equation (2.22)-Equation (2.28).

2. Dimensionalize the trajectory states, times, and angular velocity (see Section 2.3.2).

3. At each time, translate the position states from barycentric to primary-centric using Equation (2.47) (note that dimensional values should be used).

4. Define the instantaneous state rotation matrix using the second primary's Ecliptic J2000 state vector and angular momentum $\bar{h}$ (Equation (2.6)) at each time:
$$\hat{x} = \frac{\bar{R}_{P_1 \to P_2}}{|\bar{R}_{P_1 \to P_2}|}, \tag{2.53}$$
$$\hat{z} = \frac{\bar{h}}{|\bar{h}|}, \tag{2.54}$$
$$\hat{y} = \hat{z} \times \hat{x}, \tag{2.55}$$
$$^{Ec}C^{R} = \begin{bmatrix} \hat{x} & \hat{y} & \hat{z} \end{bmatrix}. \tag{2.56}$$

The full state rotation matrix can be found through the same process used in Section 2.5.1, using a dimensional angular velocity:

$$^{Ec}\dot{C}^{R} = \begin{bmatrix} n\hat{y} & -n\hat{x} & \bar{0} \end{bmatrix}. \tag{2.57}$$

in Equation (2.51) with dimensional values.

5. Nondimensionalize the states if desired.

States can be transformed from a primary-centric Ecliptic J2000 inertial frame to a barycentric rotating frame by reversing the above steps and inverting the state rotation matrix. This becomes a useful tool when designing interplanetary trajectories using multi-body dynamics.

3. CR3BP DYNAMICAL STRUCTURES

3.1 Differential Corrections

3.2 Periodic Orbits

3.3 Invariant Manifolds

4. TRAJECTORY CONSTRUCTION

4.1 2BP Lambert Arcs

4.2 The Moon-to-Moon Analytical Transfer Method

4.3 Ballistic Transfers between Earth-Moon and Sun-Earth Systems

4.4 Flyby Targeting

5. END-TO-END MARS TRANSFERS

5.1 Transfers via Intermediate Sun-Earth Halos

5.2 Direct Transfers with Flybys

6. CONCLUSION

REFERENCES

[1] K. C. Howell, "Three-dimensional, periodic, 'halo' orbits," *Celestial Mechanics*, vol. 32, no. 1, pp. 53–71, 1984. DOI: 10.1007/BF01358403.

[2] B. Semenov, *Spice: An observation geometry system for space science missions*, 2023. [Online]. Available: https://naif.jpl.nasa.gov/naif/.

[3] D. A. Vallado, *Fundamentals of Astrodynamics and Applications*, Fourth Edition. Hawthorne, CA, USA: Microcosm Press, 2013.

[4] D. C. Garcia, "Transfer design methodology between neighborhoods of planetary moons in the circular restricted three-body problem," Ph.D. Dissertation, Purdue University, West Lafayette, IN, USA, 2021.

[5] E. M. Zimovan, "Characteristics and design strategies for near rectilinear halo orbits within the earth-moon system," Ph.D. Dissertation, Purdue University, West Lafayette, IN, USA, 2017.

[6] K. K. Boudad, K. C. Howell, and D. C. Davis, "Departure and escape dynamics from the near rectilinear halo orbits in the earth-moon-sun system," *The Journal of the Astronautical Sciences*, 2022. DOI: 10.1007/s40295-022-00328-w.

[7] K. K. Boudad, "Disposal dynamics from the vicinity of near rectilinear halo orbits in the earth-moon-sun system," M.S. Thesis, Purdue University, West Lafayette, IN, USA, 2018.

[8] D. J. Scheeres, "The restricted hill four-body problem with applications to the earth-moon-sun system," *Celestial Mechanics and Dynamical Astronomy*, vol. 70, pp. 75–98, 1998. DOI: 10.1023/A:1026498608950.

[9] M. A. Andreu, "Dynamics in the center manifold around l2 in the quasi-bicircular problem," *Celestial Mechanics and Dynamical Astronomy*, vol. 84, pp. 105–133, 2002. DOI: 10.1023/A:1019979414586.

[10] M. Kakoi, K. C. Howell, and D. Folta, "Access to mars from earth-moon libration point orbits: Manifold and direct options," *Acta Astronautica*, vol. 102, pp. 269–286, 2014. DOI: 10.1016/j.actaastro.2014.06.010.

[11] J. S. Parker and R. L. Anderson, *Low-Energy Lunar Trajectory Design.* Pasadena, CA, USA: NASA Jet Propulsion Laboratory, 2013.